

Searching for Dark Matter Searches with MiniBooNE

Presented to the FNAL PAC Dec 16, 2013

The MiniBooNE Collaboration

R. Dharmapalan, & I. Stancu
University of Alabama, Tuscaloosa, AL 35487

R. A. Johnson, & D.A. Wickremasinghe
University of Cincinnati, Cincinnati, OH 45221

R. Carr, G. Karagiorgi, & M. H. Shaevitz
Columbia University; New York, NY 10027

B.C. Brown, F.G. Garcia , R. Ford, T. Kobilarcik,
W. Marsh, C. D. Moore, D. Perevalov, & W. Wester
Fermi National Accelerator Laboratory, Batavia, IL 60510

J. Grange, & H. Ray
University of Florida, Gainesville, FL 32611

R. Cooper, R. Tayloe, & R. Thornton
Indiana University, Bloomington, IN 47405

G. T. Garvey, W. Huelsnitz, W. Ketchum, Q. Liu, W. C. Louis, G. B. Mills,
J. Mirabal, Z. Pavlovic, C. Taylor, R. Van de Water, & D. H. White
Los Alamos National Laboratory, Los Alamos, NM 87545

B. P. Roe
University of Michigan, Ann Arbor, MI 48109

A. A. Aguilar-Arevalo, & I. L. de Icaza Astiz
Instituto de Ciencias Nucleares, Universidad Nacional Autónoma de México, D.F. México

P. Nienaber
Saint Mary's University of Minnesota, Winona, MN 55987

T. Katori
Queen Mary University of London, London, E1 4NS, UK

C. Mariani
Virginia Tech, Blacksburg, VA, 24061

The Theory Collaboration

B. Batell
University of Chicago, Chicago, IL, 60637

P. deNiverville, M. Pospelov, & A. Ritz
University of Victoria, Victoria, BC, V8P 5C2

D. McKeen
University of Washington, Seattle, WA, 98195

Contents

1	Executive Summary	4
2	Introduction and Motivation	6
3	Theoretical Scenario	8
3.1	Light Sub-GeV Dark Matter and Dark Forces	8
3.2	Dark Matter Production at MiniBooNE	9
4	MiniBooNE Dark Matter Detection Strategy and Sensitivities	13
4.1	Dark Matter Signal Extraction	13
4.1.1	Energy Method	14
4.1.2	Timing Method	15
4.1.3	Beam-Dump Method	16
4.1.4	Predicted NCE Nucleon Rate in Beam-Dump Mode	19
4.2	Dark Matter-Nucleon Sensitivities with Neutrino and Antineutrino Data . .	20
4.3	Dark Matter-Nucleon Sensitivities with One Week Beam Off Target Test Run	21
4.4	Projected Dark Matter-Nucleon Sensitivities with 0.35E20 POT and 1.75E20 POT in Beam-Dump	21
4.5	Dark Matter-Electron Scattering Analysis	25
5	Experiment Turn On, Test Run Goals, and Collaboration Strength	26
6	Summary	27
7	The Request	28

1 Executive Summary

The MiniBooNE experiment at the Fermi National Accelerator Laboratory (FNAL) was designed to probe neutrino oscillations at the few eV mass scale. Running for the last decade in both neutrino and antineutrino mode, MiniBooNE has successfully accomplished its primary objectives and produced measurements that support the oscillation interpretation of the LSND signal. Systematic uncertainties now dominate total measurement errors, and therefore more statistics in either neutrino or antineutrino mode will not provide significant new information on the question of oscillations.

A proposal to the FNAL PAC in 2012 [1] called attention to a new opportunity for the MiniBooNE experiment to carry out a sensitive search for light dark matter particles. Recent theoretical work has highlighted the motivations for light sub-GeV dark matter candidates that interact with ordinary matter through light mediator particles. These scenarios constitute a cosmologically and phenomenologically viable possibility to account for the dark matter of the universe. Such light dark matter particles are difficult to probe using traditional methods of dark matter detection, but can be copiously produced and then detected with neutrino beam experiments such as MiniBooNE. This represents a new experimental approach to the search for dark matter and is highly complementary to other approaches, such as underground direct detection experiments, cosmic and gamma ray satellite and balloon experiments, neutrino telescopes, and high energy collider experiments. Furthermore, searches for light dark matter provide an additional important physics motivation for the current and future experimental particle physics research program at FNAL.

In the standard beam on target configuration of MiniBooNE, a large flux of neutrinos emerges out of the proton-beryllium target collisions and are then detected through a charged or neutral current scattering signature in the large-volume electromagnetically-sensitive detector located 540m downstream. Slightly modifying the beam configuration allows the protons are steered past the target and onto the fixed 50 m absorber at the end of the decay volume. This beam-dump mode provides an ideal setup to search for low mass dark matter particles. For motivated dark matter models based on hypercharge kinetic mixing, MiniBooNE can probe parameter regions that are consistent with the observed cosmic relic abundance and explain the muon $g - 2$ discrepancy. More generally, a detailed measurement of the beam-dump Neutral Current Elastic (NCE) rate, constrained by the high statistics muon NCE to Charge-Current Quasi Elastic (CCQE) differential cross-section ratio $((d\sigma_{NCE}/dQ_{QE}^2)/(d\sigma_{CCQE}/dQ_{QE}^2))$ measured in both neutrino and antineutrino mode, will allow for a very sensitive test for possible new physics contributions, presumably from a dark sector, which is expected on general grounds to couple to the Standard Model through a neutral current-like interaction.

MiniBooNE has completed its antineutrino run, and has the capability for continued stable operation for many years. The recently strengthened collaboration is committed to running the experiment and analyzing the data in a timely manner. Extrapolating from recent proton on target (POT) rates, and assuming no technical problems, MiniBooNE could reach a total of 1.75×10^{20} POT by mid 2014 when MicroBooNE begins operation and switches to neutrino mode.

The original 2012 PAC request [1] for beam-dump running was declined. The PAC found the physics case to be motivated, but raised fair concerns regarding the remaining

collaboration resources and suggested a dark matter search analysis first be performed on the existing neutrino and antineutrino data already collected. This proposal will describe how these criticisms have been addressed. Furthermore, it will be shown that with the critical information gained from a short test run in the spring of 2012 and more recently the fall of 2013, the sensitivity to light dark matter particles can be significantly improved with a longer beam-dump run. It is estimated that with a total of 1.75×10^{20} POT in beam-dump mode deviations from the null hypothesis of the NCE rate can be detected at the 10% level, where systematic errors start to dominate. Interpreted in terms of canonical light dark matter models with kinetic mixing, this measurement can exclude an explanation of the muon $g - 2$ anomaly at the $\sim 3\sigma$ level over much of the parameter space. This new analysis leverages our detailed understanding of the $(d\sigma_{NCE}/dQ_{QE}^2)/(d\sigma_{CCQE}/dQ_{QE}^2)$ cross section ratio measured with high statistics in both neutrino and antineutrino mode, and the use of reconstructed nucleon energy and beam timing to reject backgrounds.

In the last year the intensity frontier community has recognized our experimental methods and theoretical models as being novel and worthy of pursuit. The technique of searching for light sub-GeV dark matter with proton fixed target and beam dump setups has been extensively highlighted in the Snowmass 2013, LBNE, and Project X white papers [2]. The ongoing MiniBooNE effort represents the pioneering search for light dark matter with a neutrino experiment. A run as proposed here will be the first dedicated proton beam-dump experiment with enough statistics to perform a significant analysis, resulting in new strong limits on light dark matter and publishable results. In addition, a successful execution of this proposal and a demonstration of the technique to search for light dark matter will allow current and future FNAL experiments such as MiniBooNE+, MicroBooNE, LAr1-ND, NOvA, MINERvA, and LBNE to build on the lessons learned from the MiniBooNE run and develop their own searches. The Project X proton accelerator proposal can take these searches to the next level with significantly higher anticipated proton rates. Searches for light dark matter provide a novel and important physics motivation for intense proton beam and sensitive detector facilities, which are, and will continue to be, the bedrock of the FNAL experimental program.

Using MiniBooNE to search for light sub-GeV dark matter will take a well understood experiment and put it to a new and exciting use. The search for dark matter is one of the top priorities in particle physics today, and represents one of our best indications for new dynamics beyond the Standard Model. MiniBooNE has the capability to probe a completely new range of dark matter model/parameter space. Discovery of light dark matter would revolutionize our view of the universe and would have dramatic implications for the future of particle physics and cosmology.

MiniBooNE requests running to collect a total of 1.75×10^{20} POT in beam-dump mode. This will allow a sensitive measurement of the neutral current elastic nucleon event rate in a beam configuration mode that enhances any possible non-Standard Model contribution, with significant sensitivity to specific models of light dark matter in a parameter region consistent with the required cosmic relic density an explanation of the muon $g - 2$ discrepancy. The experiment further requests that this beam be delivered in 2014 before the MicroBooNE experiment turns on.

2 Introduction and Motivation

The hypothesis of dark matter in the form of a new stable elementary particle provides a compelling and economical account of a variety of otherwise mysterious gravitational phenomena, such as the flatness of the velocity rotation curves in galaxies, the gravitational lensing of light from distant luminous sources, the amount of structure observed on large and small scales in the universe, and the precisely measured temperature anisotropies in the cosmic microwave background radiation. Indeed, the evidence for dark matter provides one of the strongest motivations for new particle physics beyond the Standard Model. A dedicated experimental program has emerged over the past two decades to detect the non-gravitational interactions of dark matter with ordinary matter, including searches in underground direct detection experiments, cosmic and gamma ray satellite and balloon experiments, neutrino telescopes, and high energy collider experiments.

It has recently been demonstrated [5, 6, 7] that neutrino beam experiments, and MiniBooNE in particular, have significant potential to search for light sub-GeV mass dark matter particles. The basic experimental principle is analogous to neutrino detection: light dark matter particles are produced in the primary proton-target collisions and subsequently travel to the near detector downstream and scatter with electrons or nuclei, leaving a neutral current-like signature. This method of searching for dark matter is complementary to the approaches cited above and provides the best sensitivity to light dark matter below a few GeV in mass interacting with quarks through a light mediator. The exciting prospect of searching for dark matter in this manner gives important new motivation to the FNAL experimental particle physics program at the intensity frontier, as experiments such as MiniBooNE, MINOS, MiniBooNE+, MicroBooNE, LAr1-ND, NOvA, MINERvA, and in the future, LBNE and Project X all have the potential to carry out searches for dark matter.

This proposal summarizes the physics case and technical feasibility for a dedicated dark matter search at MiniBooNE in a beam-dump run configuration. As we will describe in detail below, this run mode substantially reduces the neutrino flux, and thus the rate of neutral current neutrino scattering, which constitutes a primary background to the dark matter signal. With 1.75×10^{20} POT a highly sensitive search for sub-GeV dark matter can be carried out that will allow MiniBooNE to probe new regions of parameter space, and for certain motivated models of dark matter, will provide the best sensitivity.

An important ingredient of realistic light dark matter models is the presence of light sub-GeV *mediator* particles that couple dark matter to ordinary matter [16, 17, 18] (see also [19]). In the canonical thermal freezeout scenario, such light mediators are generally required to open up new annihilation channels in the early universe in order for light dark matter to achieve the required relic abundance and evade the so-called Lee-Weinberg bound [15]. In asymmetric dark matter scenarios [8], light mediators are generically invoked to deplete the symmetric dark matter component. While essential for a viable cosmology, light mediators are also clearly desirable from a phenomenological perspective as they mediate dark matter production and scattering channels that can be exploited by low energy, high intensity experiments. In particular, at neutrino experiments such as MiniBooNE, light mediator particles will be produced in the proton-target collisions and subsequently decay to dark matter particles, thus supplying a relativistic source of dark matter particles which can be detected via elastic scattering on nuclei or electrons in the near detector.

Light dark matter and light mediator particles have been the subject of intense theoretical and experimental investigation in recent years. MeV-mass dark matter was originally proposed [13] to account for the via annihilation a strong diffuse 511 keV emission from the galactic bulge. Vector and scalar boson mediators with sub-GeV masses can also reconcile the discrepancy in measured and calculated values of $g - 2$ of the muon [20, 21]. Furthermore, such mediators have received attention as a possible explanation of the proton charge radius discrepancy [23]. Therefore, both light dark matter particles and light mediators are of considerable interest as possible explanations for various puzzles in both astrophysics and particle physics. More broadly, searches for dark sectors and new light weakly coupled particles has developed into a rich subfield of intensity frontier physics and was recently prominently featured during the Snowmass community planning exercise [2] (see also [24],[22]).

The original PAC proposal [1] highlighted the benefits of running MiniBooNE in a beam-dump mode, in which the 8.9 GeV proton beam is steered off target and directed into the absorber at the end of the decay pipe. In this configuration, the neutrino flux can be reduced by about a factor of 71, while the dark matter production is unchanged. This setup significantly reduces neutrino neutral current backgrounds that can mimic the scattering of dark matter off nucleons or electrons. Since the last PAC proposal, MiniBooNE has utilized new information gained from two short test runs in beam-dump mode to better understand the dominant backgrounds to the dark matter signal in beam-dump mode, allowing for an accurate projection of dark matter parameter space as a function of POT.

It must be emphasized that MiniBooNE has a distinct advantage in carrying out a search of this kind: we can capitalize on the effort expended during the last decade in understanding the detector response and the standard backgrounds – in particular, those coming from the dirt surrounding the detector or cosmic rays. A robust and well-tested particle identification tool-set is at our disposal and will be utilized in the dark matter search. Furthermore, MiniBooNE has performed a number of high-statistics neutrino cross section measurements in both the neutral current and charged current channels [25, 26, 27, 28, 29, 30, 31, 32, 33, 34]. Indeed, the experiment has measured the cross sections for 90% of the neutrino interactions in MiniBooNE. A new light dark matter search experiment would require a significant investment of time and manpower to achieve a similar understanding of the detector and the backgrounds.

The proposed search will probe dark matter/mediator masses in the range of 10 - 250 MeV. We will present an interpretation of the search for a canonical scenario in which hypercharge kinetic mixing is responsible for mediation. For this model, the beam-dump search will cover new regions of dark matter parameter space at the higher end of this mass range. Furthermore, for certain values of the dark sector gauge coupling, this search can definitively test a possible explanation of the muon $g - 2$ discrepancy. It should be emphasized that other dark matter models exist in which the mediator couples dominantly to quarks, and for such models the MiniBooNE search will have unique sensitivity. Furthermore, the knowledge and experience gained with this run will prove invaluable for future dark matter searches with NO ν A, MINER ν A, MicroBooNE, LBNE and Project X.

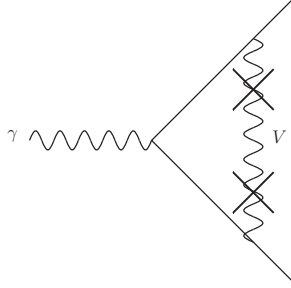


Figure 1: The contribution to the anomalous magnetic moment of SM fermions from the vector mediator. The crosses represent the kinetic mixing κ of the vector V with the photon.

3 Theoretical Scenario

3.1 Light Sub-GeV Dark Matter and Dark Forces

Minimal sub-GeV dark matter models are characterized by the mass scale and interaction strengths of the dark matter particle and the mediator that controls the coupling to ordinary matter. General effective field theory arguments suggest that the dominant interactions of a gauge singlet mediator will be through renormalizable couplings, of which only three are possible in the Standard Model – the so-called “portal” interactions. Within models utilizing portals to mediate interactions, a fairly systematic exploration of the constraints on the various dark matter–mediator combinations is possible. Sub-GeV dark matter models are subject to a variety of cosmological, astrophysical, and particle physics constraints, as discussed *e.g.* in [6, 7, 2]. With minimal model assumptions, these constraints single out a massive U(1) vector V^μ as the most viable candidate for the mediator particle, which couples to the Standard Model through kinetic mixing with the hypercharge gauge boson [35]. At energy scales below the weak scale, this ultimately leads to kinetic mixing with the photon, $\mathcal{L}_{\text{mix}} = \frac{\kappa}{2} F_{\mu\nu} V^{\mu\nu}$. Moreover, light dark matter is strongly constrained by the impact of annihilation on the cosmic microwave background radiation (CMB), which can distort the well measured temperature and polarization anisotropies. Thus, for a viable thermal freezeout cosmology, the dark matter candidates should exhibit p -wave annihilation in low-velocity regimes. This selects a complex scalar χ charged under the new U(1) vector as a natural light dark matter candidate. Therefore, the benchmark model we consider takes the form [6, 7],

$$\mathcal{L}_{\text{DM}} = V_\mu (e\kappa J_{\text{em}}^\mu + e' J_\chi^\mu) + \mathcal{L}_{\text{kin}}(V, \chi) + \dots \quad (1)$$

on using $\partial_\mu F^{\mu\nu} = eJ_{\text{em}}^\nu$, with the electromagnetic current $J_{\text{em}}^\mu = Q_f \bar{f} \gamma^\mu f + \dots$, to rewrite the kinetic mixing interaction, $\frac{\kappa}{2} F_{\mu\nu} V^{\mu\nu}$. $J_\chi^\mu = i(\chi^\dagger \partial^\mu \chi - \partial^\mu \chi^\dagger \chi) + \mathcal{O}(V^\mu)$ is the corresponding U(1) current for scalar dark matter, with gauge coupling $e' \equiv \sqrt{4\pi\alpha'}$. In what follows, we assume small mixing κ , perturbative $\alpha' \sim 0.1$, and that $m_V > 2m_\chi$. The latter assumption determines the mass hierarchy of experimental interest for MiniBooNE and implies that $V \rightarrow 2\chi$ is the primary decay mode of the mediator. Demanding that χ is a thermal relic (i.e. with its relic abundance tied to the measured value through thermal freeze-out¹), leads

¹The dominant annihilation process in this regime is $\chi\chi^* \rightarrow V^* \rightarrow \text{SM states}$ and is viable for $m_\chi < m_V$. For larger (sub-GeV) χ masses, the dominant annihilation proceeds via $\chi\chi^* \rightarrow VV$, which is an s -wave

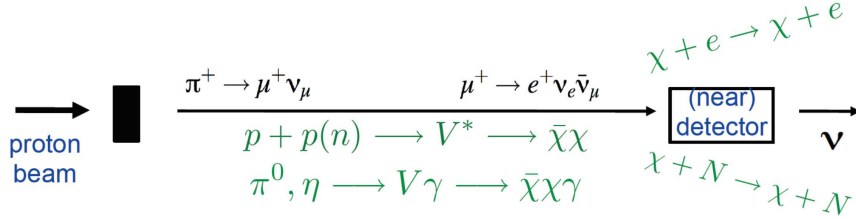


Figure 2: A schematic of the dark matter production mechanisms and elastic scattering signatures.

to a constraint on the four model parameters $\{m_\chi, m_V, \kappa, \text{ and } \alpha'\}$. One motivation for the slightly larger values $\alpha' \sim 0.1 > \alpha$ is the annihilation is more efficient, and allows more of the parameter space to avoid the overclosure constraint.

The model described above provides a simple, viable benchmark scenario and will be used in this proposal to provide a dark matter interpretation of the search sensitivities. The particular model is rather unique in its ability to escape a number of particle physics and astrophysics constraints with minimal model complexity. Furthermore, the light vector boson mediator gives a contribution through kinetic mixing to the anomalous magnetic moments of SM fermions, as depicted in Fig. 1, and can account for the current 3σ discrepancy in the muon $g - 2$ [20, 21].

While this scenario is viable and motivated, various modifications of the above framework are plausible, and other scenarios with phenomenologically distinct signatures can be constructed. It should be emphasized many of the constraints are model dependent, and rely in particular to the coupling of the mediator to leptons. On the other hand, MiniBooNE and other proton-beam experiments explicitly probe the coupling of the mediator to quarks, and in a model-independent fashion provide the best opportunity to probe this particular coupling. Thus, in light dark matter scenarios with leptophobic mediators, MiniBooNE will by far provide the best coverage [9].

3.2 Dark Matter Production at MiniBooNE

At proton fixed target and beam dump experiments, there are two main production modes for χ , where we assume $m_V > 2m_\chi$ so that (for $\alpha' \sim 0.1$ and small kinetic mixing κ) the on-shell decay $V \rightarrow 2\chi$ has a branching ratio close to unity. The first channel involves direct parton-level processes such as $p + p(n) \rightarrow V^* \rightarrow \chi^\dagger\chi$. The second channel proceeds through decays of mesons with large radiative branching such as π^0 and η in the form $\pi^0, \eta \rightarrow V\gamma \rightarrow \chi^\dagger\chi\gamma$. The produced dark matter particles travel to the detector and can be detected via elastic scattering on nucleons or electrons in the detector, as the signature is similar to the neutral current scattering of neutrinos. The basic experimental principle is illustrated in Fig. 2.

The most important production channels at MiniBooNE are via π^0 and η which subsequently decay to vector mediators that in turn decay to dark matter particles. The dark matter can then scatter on the electrons or nuclei in the MiniBooNE detector. This process is shown in Fig. 3. We estimate the π^0 and η production rate by averaging and scaling [7] the π^+ and π^- Sanford-Wang distributions used in Ref. [36] and apply the cuts from the

process and can distort the CMB.

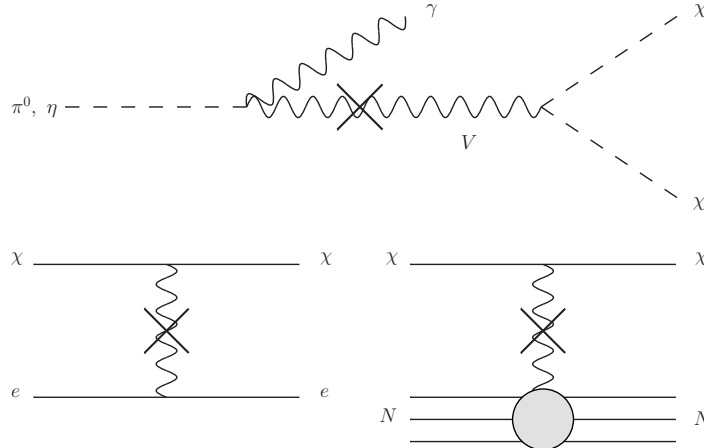


Figure 3: Top: The production of a pair of dark matter particles through neutral meson decay. Bottom: The scattering of dark matter in the MiniBooNE detector. The cross represents the kinetic mixing between the vector boson mediator V_μ and the photon.

analysis of neutral current scattering (on nucleons) in Ref. [36] to obtain a total efficiency of about 35%. (Similar efficiencies were adopted in analyzing electron scattering.) Contours in the parameter space of the hypercharge mixing dark matter model were calculated corresponding to 1, 10, and 1000 neutral current-like scattering events on nucleons or electrons with 1.75×10^{20} POT at MiniBooNE. While the Sanford-Wang parameterization employed corresponds to a beryllium target, the results are not expected to differ much when steering the beam into the iron beam dump since the ratio of the charged hadron production (which determines the number of neutrinos produced) to neutral hadrons (which determines the number of dark matter particles produced) is not strongly dependent on atomic number.

In Fig. 4, these contours are displayed in the plane of direct-detection scattering cross section σ_N vs dark matter mass m_χ for $m_V = 300$ MeV and $\alpha' = 0.1$. The cross-section σ_N describes the non-relativistic spin-independent coherent scattering on nuclei relevant for direct detection experiments, and is to be distinguished from the actual dark matter-nucleon elastic scattering cross-section at MiniBooNE. However, the translation allows the MiniBooNE sensitivity to be easily compared to direct detection experiments, whose sensitivity weakens dramatically at low dark matter mass (we display the best limits from CRESST [42] and XENON10 [43]). We also show the existing particle physics constraints on the model parameters. It is worth noting that the region in which the $(g-2)_\mu$ discrepancy is alleviated overlaps with the required relic density and with a potentially large number of dark matter scattering events at MiniBooNE.

It is interesting to compare this scenario, in which the light vector decays to dark matter particles, with the “dark force” scenario [22, 23, 24], in which the vector instead decays dominantly to the Standard Model. Such a comparison is easiest in the κ vs m_V plane for fixed dark matter mass. This parameter space is shown in Fig. 5, for the two regimes that can be alternately characterized as ‘invisible’, with $m_V > 2m_\chi$ so that V decays invisibly to dark matter, and ‘visible’ with $m_V < 2m_\chi$ so that V decays to light SM particles. The dominant decays of the vector to dark matter weakens many of the otherwise strong constraints (see

Fig. 5 for additional details). In Fig. 6, the MiniBooNE sensitivity contours are displayed in the κ vs m_V plane for $m_\chi = 10$ MeV and $\alpha' = 0.1$. Again, there is an interesting coincidence between the regions of parameter space where MiniBooNE is sensitive and those that solve the $(g - 2)_\mu$ discrepancy and give the required relic density.

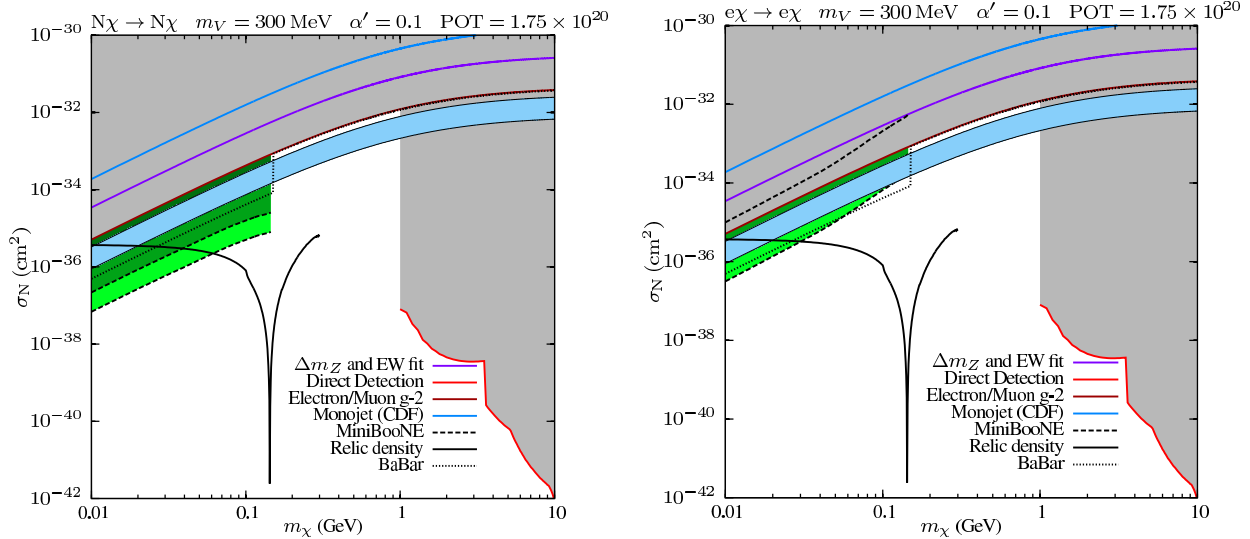


Figure 4: Regions of dark matter-nucleon scattering cross section (corresponding to non-relativistic spin-independent coherent scattering on nuclei) vs dark matter mass. In this plot we have fixed $m_V = 300$ MeV and $\alpha' = 0.1$. Constraints are shown from monojet searches ($pp \rightarrow j + \text{inv.}$) [44], excessive contributions to $(g - 2)_\mu$ [21], precision electroweak measurements [38], a monophoton search ($e^+e^- \rightarrow \gamma + \text{inv.}$) [39, 40, 41] (labeled BaBar), and low-mass limits from dark matter direct detection experiments, DAMIC [46] (1-3 GeV), CDMSlite [47] (3-5 GeV) and XENON10 [43] (5-10 GeV). Note that a slightly stronger exclusion contour to XENON10 has recently been obtained by LUX [48]. The light blue band represents the region where the current $\sim 3\sigma$ discrepancy in $(g - 2)_\mu$ is alleviated by the 1-loop contribution from the vector mediator [21]. The solid black line indicates where the relic density of the dark matter matches observations—the structure in this contour is due to s -channel V^* resonant enhancement in the dark matter annihilation cross section for $m_\chi \sim m_V/2$. For $m_\chi > m_V$, new annihilation channels open up and this relation is modified. The left panel shows regions where we expect 1–10 (light green), 10–1000 (green), and more than 1000 (dark green) elastic scattering events off nucleons in the MiniBooNE detector with 1.75×10^{20} POT. The right panel shows the same for elastic scattering off electrons.

The dark matter and vector masses chosen in Figs. 4,5,6 are representative in that the dark matter production at MiniBooNE is not strongly sensitive to choices of mass provided the mediator can be produced in the decays of light mesons, $m_V < m_\eta$, and it decays invisibly, i.e. $m_V > 2m_\chi$. Moreover, while the potential MiniBooNE sensitivity is illustrated here for the model of light scalar χ particles interacting through a kinetically mixed vector boson, the experimental results obtained in such a study could easily be interpreted in the context of other models of sub-GeV dark matter and light mediators in a similar kinematic range.

There are two important existing experimental constraints on this particular model. One constraint, relevant for low masses $2m_\chi < m_V < m_{\pi^0}$, comes from the LSND measurement of the neutrino-electron elastic scattering cross section [6, 51]. Another constraint, which is important for larger vector masses, comes from a BaBar search for the monophoton signature [39, 40, 41]. Taken together, these two constraints exclude a possible explanation of

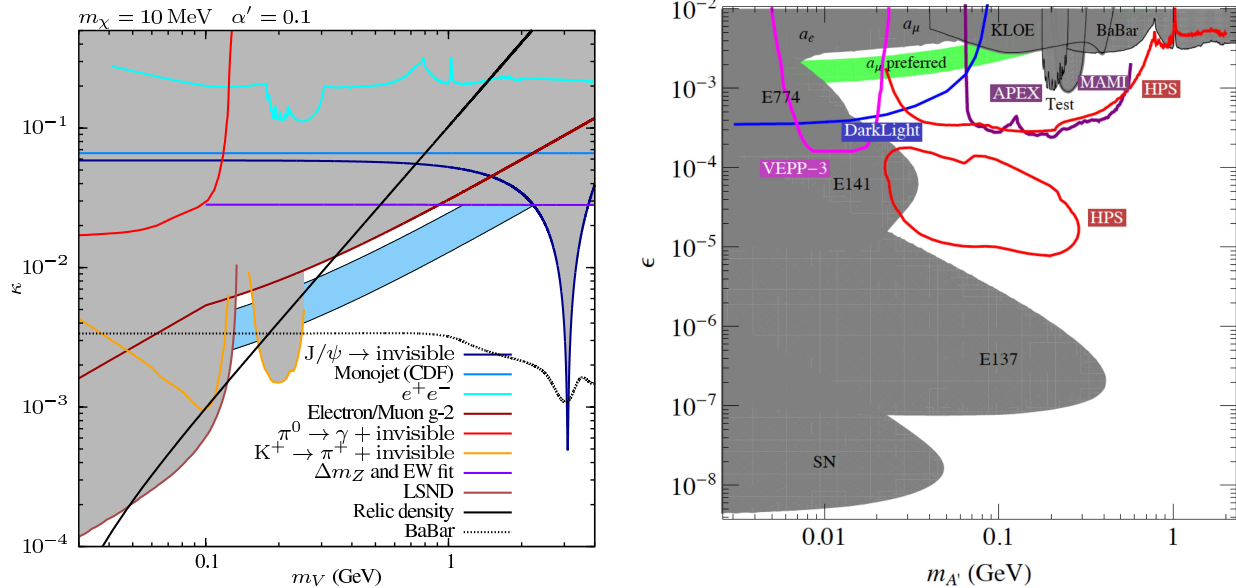


Figure 5: Regions of kinetic mixing parameter κ (ϵ) vs vector mass m_V ($m_{A'}$), contrasting the existing sensitivity to light vectors in the two scenarios where the dominant decay mode of the vector is either visible or invisible. On the left we show the sensitivity to the light dark matter model considered here, in which $m_V > 2m_\chi$ so that the vector predominantly decays invisibly and $\text{Br}(V \rightarrow \text{SM}) \sim \kappa^2 \alpha' / \alpha$ with $\alpha' = 0.1$. On the right (reproduced from [24], figure courtesy of R. Essig), this is contrasted with the sensitivity in the absence of light dark matter, or with $m_V < 2m_\chi$, so that $\text{Br}(V \rightarrow \text{SM}) \sim \mathcal{O}(1)$. The shaded regions are existing limits, while the open contours are current and planned searches. Note that in the light dark matter scenario, many of the existing dark force constraints shown on the right are weakened by the reduced leptonic branching ratio, while beam dump limits that rely on a long lifetime for the V are removed entirely. In the left-hand plot, as in Fig. 4, constraints from dark force searches (labeled e^+e^-) [24], the LSND neutrino - electron elastic scattering measurement [6, 51], $pp \rightarrow j + \text{inv.}$ [44] (labeled Monojet), $e^+e^- \rightarrow \gamma + \text{inv.}$ [39, 40, 41] (labeled BaBar), $J/\psi \rightarrow \text{inv.}$ decays [45], and excessive contributions to $(g-2)_\mu$ [21] are shown, along with limits from $\pi^0 \rightarrow \gamma + \text{inv.}$ [49] and $K^+ \rightarrow \pi^+ + \text{inv.}$ [50] decays. The light blue band again indicates the region where the current $\sim 3\sigma$ discrepancy in $(g-2)_\mu$ is alleviated [21], and the solid black line shows the parameters required to reproduce the observed relic density of dark matter.

the muon $g-2$ anomaly in this model at 95% C.L., except for vector masses slightly above the pion mass (see Fig. 6). MiniBooNE can cover the remaining $(g-2)_\mu$ motivated region for values of α' larger than about 0.1 with a similar confidence. However, it is important to emphasize two points regarding $(g-2)_\mu$: 1) while $(g-2)_\mu$ provides an interesting “target” in the parameter space of this particular dark matter model (to which MiniBooNE is sensitive), the primary motivation for these searches is as a novel and powerful probe of a generic class of light dark matter scenarios, which extends beyond any muon $(g-2)_\mu$ motivation. 2) The strong constraints from LSND and the BaBar search rely on the coupling of the mediator to leptons, and if instead the mediator couples only to quarks at a substantial level, MiniBooNE and other proton beam experiments will have superior sensitivity.

We also wish to contrast the MiniBooNE sensitivity with monojet searches at the Tevatron and the LHC, as both rely only on the coupling of the mediator to quarks. One can notice from Fig. 4 that MiniBooNE has far superior sensitivity in this model. In fact, this conclusion holds in general provided the dark matter interacts with the Standard Model through a light, (sub-)GeV scale mediator, and can be understood as follows. In the light

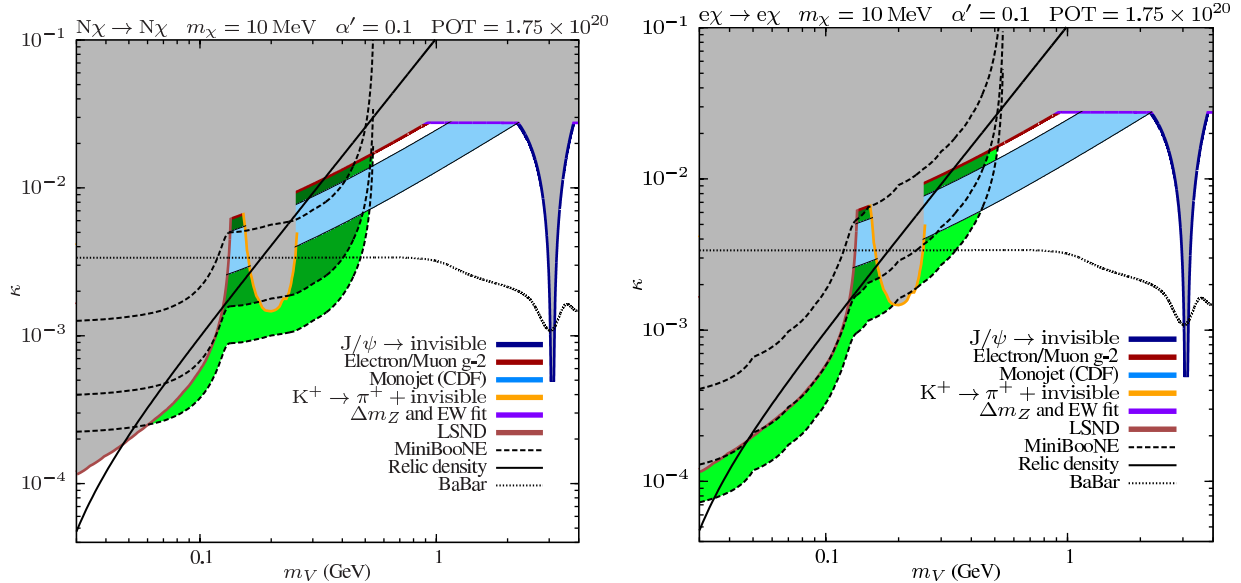


Figure 6: Regions of mixing angle κ vs vector mass m_V , showing the MiniBooNE sensitivity contours for the light dark matter scenario. The contours assume a dark matter mass $m_\chi = 10$ MeV and $\alpha' = 0.1$. The existing limits are as in Fig. 5, while the solid black line again shows the parameters required to reproduce the observed relic density of dark matter. The left panel shows regions where we expect 1–10 (light green), 10–1000 (green), and more than 1000 (dark green) elastic scattering events off nuclei in the MiniBooNE detector with 1.75×10^{20} POT. The right panel shows the same for elastic scattering off electrons. The green lobes showing enhanced sensitivity at lower mass are the result of vectors produced in π^0 decays while the right lobes show those from η decays.

mediator limit, the production cross section hadron colliders will fall as $1/E^2$, where E is the characteristic energy involved in the collision (in practice this is roughly the transverse momentum cut employed on the hard jet in the event). Thus, in the case of a light mediator, the rate is suppressed at high energy colliders as the typical collision energies are higher. On the other hand, in the opposite regime of a heavy mediator or contact operator, the production cross section will scale as E^2/M^4 , with M the mass of the mediator (or suppression scale in the higher dimensional operator). Thus, high energy collisions yield the highest production rate, and in this regime LHC will provide the best sensitivity. Refs. [44, 52] consider in detail the monojet constraints on light dark matter interacting through a light mediator.

4 MiniBooNE Dark Matter Detection Strategy and Sensitivities

4.1 Dark Matter Signal Extraction

Once produced in the beam, dark matter can travel the ~ 500 m distance through rock to interact in the detector. The main detection channel is neutral current elastic like scattering off nucleons or electrons in the mineral oil (CH_2). To first order, dark matter scattering will look like neutrino neutral current scattering, though with different kinematics. MiniBooNE has already published results on NCE nucleon scattering cross section in both neutrino and

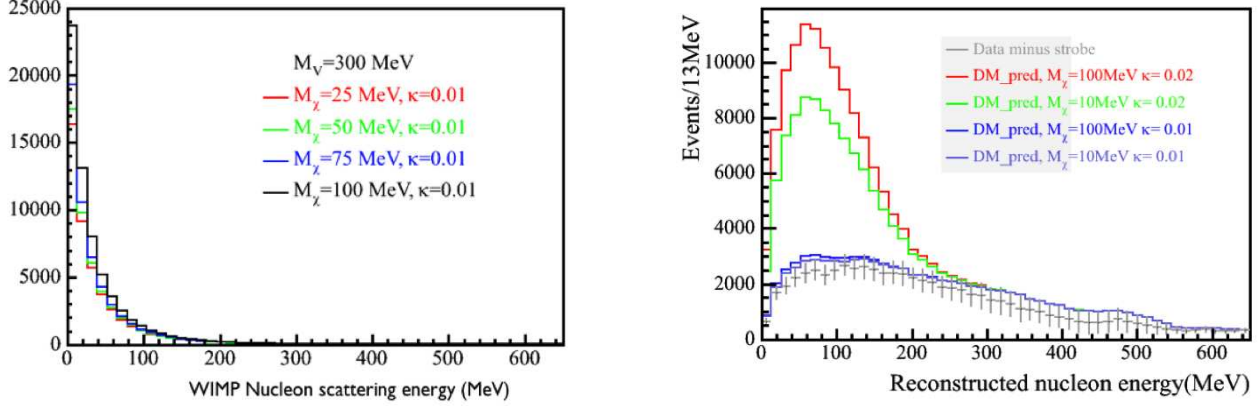


Figure 7: Nucleon kinetic energy from dark matter scattering for various model parameters (left). Reconstructed nucleon kinetic energy for both dark matter and neutrino scattering after corrected for detector efficiency (right).

antineutrino mode, demonstrating that measurements of this type of process are possible [27, 28]. Measurements of neutrino electron elastic scattering were performed and were reported in a thesis [53].

In both cases, searching for dark matter-like signals will have to contend with the dominant neutrino scattering background both from inside and outside (dirt) the tank, and beam unrelated cosmics. Therefore, any technique that can significantly reduce or constrain these backgrounds will improve the sensitivity of the search. Four main methods employed are:

1. Energy spectrum shape differences to extract signal.
2. Event timing relative to the beam to look for sub-luminal dark matter particles, or to reject out of time cosmic and dirt backgrounds.
3. Beam-dump running to significantly reduce the neutrino.
4. NCE nucleon constraint from the high statistic $(d\sigma_{NCE}/dQ_{QE}^2)/(d\sigma_{CCQE}/dQ_{QE}^2)$ cross sections applied to the observed CCQE muon rate in beam-dump mode.

4.1.1 Energy Method

Dark matter-nucleon scattering events to first order look like neutrino nucleon neutral current scattering. However, due to the kinematics of the dark matter production, it can produce a nucleon kinetic energy spectrum different than those from neutrinos. Figure 7 shows the dark matter kinetic energy, which peaks at low energy, for various model parameters. Also shown is the resulting nucleon kinetic energy after it has been corrected for detector efficiency, and overlaid on the neutrino NCE data. It is clear that differences in the kinetic energy are apparent, with dark matter scattering occurring mostly below 250 MeV, and independent of model parameters. Thus fitting with dark matter-nucleon energy templates will improve the overall sensitivity.

4.1.2 Timing Method

The dark matter mass region where MiniBooNE is sensitive is from 10 MeV up to about 200 MeV. Given the ~ 500 m travel distance of the dark matter particles from the production point to the detector, and the few nanoseconds absolute timing resolution of the detector relative to the proton beam, we have the ability to separate out neutrino events that travel at the speed of light from dark matter with masses above ~ 70 MeV. This allows better signal to background rejection and improves detection sensitivities.

Figure 8 shows a simple drawing of dark matter production and detection relative to the various experiment components. A key criterium is that protons range out in the iron absorber in ~ 1 m and the π^0 and η , which the dark matter particles couple to, decay promptly on the order of 10^{-16} seconds. This localizes spatially and temporally the production point of the dark matter. The produced dark matter particles then travel to the detector at a velocity based on their mass and momentum. Figure 9 shows the relationship between dark matter mass and timing delay for an assumed momentum of 1.5 GeV, which is the mean momentum for typical production kinematics with the 8.9 GeV proton beam.

Absolute NCE nucleon event timing relative to the Resistive Wall Monitor (RWM) beam signal can be reconstructed using the timing signal from the beam crossing delivered to the detector via the 540 m cable. There are 81 RF buckets (53MHz) that contain the protons, and the detector timing is synchronized to this RF beam structure. After various corrections applied to the buckets, the detector event timing relative to the RWM can be reconstructed with the 81 RF buckets overlaid on top of each other to make one profile. Figure 10 shows a plot of the reconstructed NC nucleon timing relative to the RWM signal. Events far out on either side of the Gaussian centroid can be considered out of time, i.e. these are events that fall within the 53 MHz buckets, and are out of time either early or late, though we will assume they are late for this analysis. Also shown in the plot are the various backgrounds and their time distributions. The NCE and NCE-Bkg (these are NCE events where the pion is absorbed) events are due to neutrino interactions and are in time with the beam RF structure. The cosmic beam unrelated background (strobe) and dirt (due to neutrino interactions in the rock) are both flat in time. For cosmic events this is due to the fact that they occur randomly relative to the beam. Dirt events are from the beam, however, they are produced outside the detector in the surrounding rock and due to mass time of flight delay and/or geometrical effects (production at right- or backward-angles), they become out of time relative to the beam.

Timing reconstruction studies indicate that the time resolution achievable is ~ 1.8 nsec for CCQE muon events and ~ 4.2 nsec for NCE events. The larger time resolution for NCE is due to these events being dominated by scintillation light, which is slower, compared to CCQE muon Cerenkov prompt light. In Figure 10 one can see that in-spite of the larger resolution, there is still useful timing information. For instance, the fact that the data and background agree in the out-time region (0-4 and 16-20 nsec) where the cosmic and dirt backgrounds dominate indicates that these rates are properly estimated. The cosmic backgrounds are much more significant during beam-dump running, hence the timing is more crucial for this run mode. For instance, looking at events in the in-time region enhances the neutrino NCE events while rejecting dirt and cosmic backgrounds, which in beam-dump mode, are the dominate backgrounds. If we reverse the cuts, we then can study an enriched sample of dirt

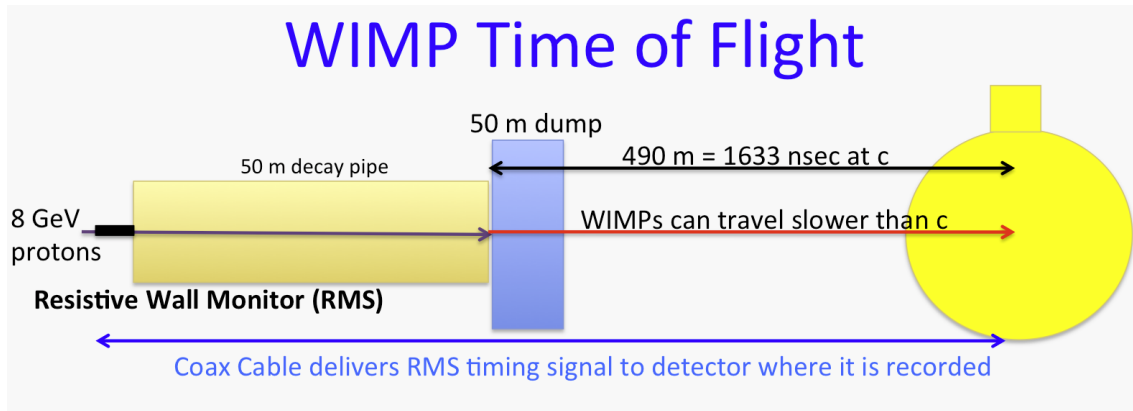


Figure 8: Simple timing drawing showing the production and reconstruction of events.

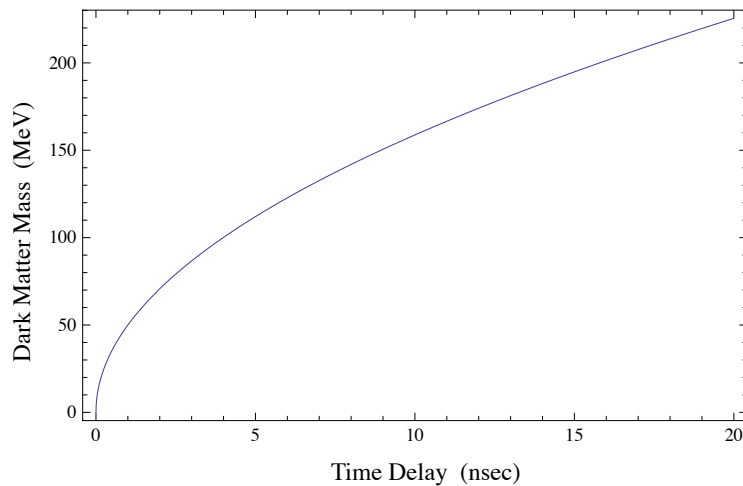


Figure 9: Dark matter mass versus time delay for an average dark matter momentum of 1.5 GeV.

and cosmics. Should we find an excess in either of these regions, it can give us important clues as to its origin and significance.

Ultimately, fitting to dark matter-nucleon timing templates will give the best sensitivity. Work is in progress on this method and could be presented at the PAC meeting.

4.1.3 Beam-Dump Method

Dark matter scattering signals in the MiniBooNE detector to first order resemble neutrino neutral current scattering. The number of neutrino induced background events are in the thousands per 1×10^{20} POT, and would make searches for small dark matter signals extremely difficult. A method is proposed that will reduce the neutrino flux by up to two orders of magnitude, making sensitive searches achievable.

Dark matter production is via the vector mediator coupling to the photons in π^0 and η decay. In beam-dump running, the protons interacting in the Fe absorber produce neutral mesons, to first order, at the same rate as in Be. Furthermore, since they decay quickly

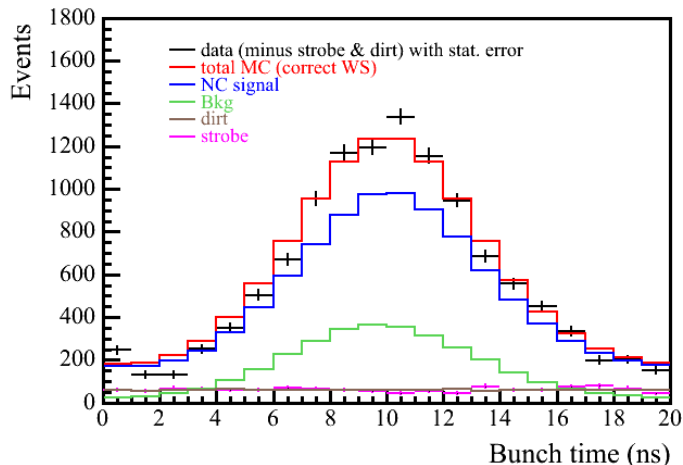


Figure 10: Reconstructed antineutrino NCE nucleon timing relative to the beam for both data and absolutely normalized Monte Carlo. The individual backgrounds do not add up to the total MC due to various weights applied for wrong-sign contributions. In-time is defined from 4-16 nsec, and out-time from 0-4 and 16-20 nsec.

($\sim 10^{-16}$ sec) they are not absorbed and hence can still produce dark matter at a rate that only scales with protons on target.

The neutrino flux can be significantly reduced by pointing the beam past the target where it then travels through air to the 50 m iron absorber, or 25 m iron absorber if deployed. There is a 1 cm air gap around the target between the Be and the inner horn conductor. Since the beam spot is 1 mm in size, there is ample room to safely point the beam past the target. The interaction length for 8.9 GeV protons in air at atmospheric pressure is about 1 km, so that 50 m is about a 5% interaction length.

When the protons impact the iron absorber, the charged mesons quickly range out in the dense iron and are absorbed, thereby preventing the decay that produces neutrinos. The few charged mesons that are produced in the air or in the iron absorber and decay are not focused and hence the neutrinos do not gain from the horn focusing, again reducing the flux at the detector. Monte Carlo simulations show in Figure 11 the flux reduction relative to normal neutrino mode running. Integrating the flux reduction over all energies above 0.3 GeV, one obtains the Monte Carlo prediction for the muon neutrino flux reduction ratio:

$$\frac{\text{Flux (events/POT)}^{\nu \text{ mode}}}{\text{Flux (events/POT)}^{\text{beam-dump mode}}} = 67. \quad (2)$$

Since November 8, 2013, the BNB has been delivering test beam in beam-dump mode to the 50 m absorber. The MiniBooNE detector is on and taking data as part of a short (4-6 weeks) test run to collect enough statistics to determine important inputs to the analysis. With three weeks of data collected, for a total of 1.8×10^{19} POT, we are able to determine the reconstructed CCQE muon neutrino rate reduction relative to neutrino mode:

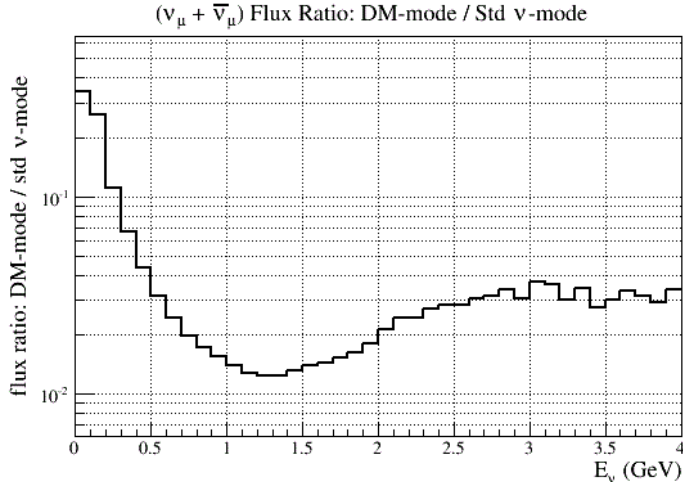


Figure 11: Muon Neutrino+Antineutrino flux reduction in beam-dump mode relative to normal neutrino mode as a function of neutrino energy.

$$\frac{\text{Rate (events/POT)}^{\nu \text{ mode}}}{\text{Rate (events/POT)}^{\text{beam-dump mode}}} = 71 \pm 6. \quad (3)$$

The Monte Carlo flux reduction ratio is close to the measured rate reduction value. However, slight differences are expected as the flux ratio does not include the effects of cross sections and detection efficiency, which the rate measurement includes. Figure 12 shows the reconstructed muon CCQE data overlayed on the Monte Carlo prediction. The agreement as a function of neutrino energy is within statistics. A final important point is that in beam-dump mode the Monte Carlo predicted neutrino rate is 73% and the antineutrino rate 27% of the total. We assume an error of 50% on the antineutrino contribution.

In the previous PAC 2012 proposal, we reported a suppression ratio of 42. The difference from here is due to the horn being turned off for the fall 2013 beam-dump test run, while the 2012 beam-dump test run had the horn turned on (for technical reasons). Beam spray up-stream from the target and horn in the beam line components produce mesons that travel down the beam pipe and focused by the horn. Monte Carlo studies confirm this scenario and are consistent with the observe rate difference. Any mention in this proposal off beam-dump mode implies horn-off, unless stated otherwise.

For sensitivities studies here we will assume beam-dump, horn off, and 50 m absorber measured reduction rate of 71 with respect to neutrino mode. By deploying the 25 m absorber, the flux reduction is increased by a further factor of two. This is to be expected since all the neutrino production is from proton interactions in air within the 50 m decay pipe. If we reduce the path length in air by a factor of two ($50m/25m$), then the neutrino rate is reduced by the same factor. This extra neutrino reduction is important for improving dark matter-nucleon scattering sensitivity for the same POT, and should be considered for systematic checks if a signal is found, or for future potential beam-dump runs with MiniBooNE+, MicroBooNE, and LAr1-ND.

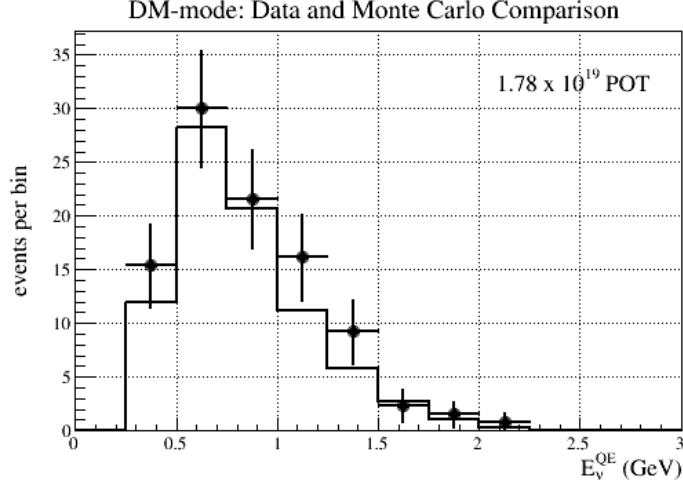


Figure 12: Reconstructed CCQE muon neutrino event rate for 1.8×10^{19} POT beam-dump mode (statistical error bars). The solid blue line is the absolutely normalized Monte Carlo prediction, showing good agreement with data. The reconstructed neutrino energy depends on the lepton visible energy and angle with respect to the beam.

4.1.4 Predicted NCE Nucleon Rate in Beam-Dump Mode

In beam-dump mode, the predicted NCE event rate can be reliably estimated by taking advantage of the high statistics measurement of $(d\sigma_{NCE}/dQ_{QE}^2)/(d\sigma_{CCQE}/dQ_{QE}^2)$ in both neutrino and antineutrino mode [27, 28]. Figure 13 shows the measurements made by Mini-BooNE in these two modes. The errors are dominated by systematics, which range from 5% to 10% below a Q^2 of 0.5 GeV^2 .

The CCQE muon neutrino rate as a function of reconstructed neutrino energy can be reliably estimated as shown in Figure 12. The neutrino energy can be translated to $Q_{CCQE}^2 = 2E_{QE}E_{total}(1 - \cos(\theta))$, where $\cos(\theta)$ is the angle of the muon relative to the beam direction. The nucleon Q_N^2 can be related to the nucleon mass (m_N) and its reconstructed kinetic energy (T_N) via, $Q_N^2 = 2m_N T_N$. To give some scale, the maximum nucleon kinetic energy from dark matter scattering in the model presented here is approximately 250 MeV, which corresponds to a $Q^2 = 0.47 \text{ GeV}^2$. Thus, in bins of Q^2 , we can multiply the observed CCQE muon event rate by $(d\sigma_{NCE}/dQ_{QE}^2)/(d\sigma_{CCQE}/dQ_{QE}^2)$ to determine the NCE nucleon event rate.

Since the cross section ratio is measured from data, we can use the statistical errors. The dominant errors in estimating the NCE nucleon rate will come from two sources. First, the statistics on the observed muon CCQE rate for 1.75×10^{20} POT is expected to be 1030 events, or a 3.1% flux statistical error (7.1% for 0.35×10^{20} POT). Second, the error in the cross section ratio is due to the uncertainty in the relative fraction of neutrinos and antineutrinos in beam-dump mode. The error on $(d\sigma_{NCE}/dQ_{QE}^2)/(d\sigma_{CCQE}/dQ_{QE}^2)$ is estimated to be 8.5%. Adding these two errors in quadrature gives a total systematic error of 9% for 1.75×10^{20} POT and 11.1% for 0.35×10^{20} POT. The biggest impact on the sensitivity is the five times increase in the NCE data, which will reduce the statistical errors on the backgrounds from 9.2% to 4.1%, where they are no longer significant.

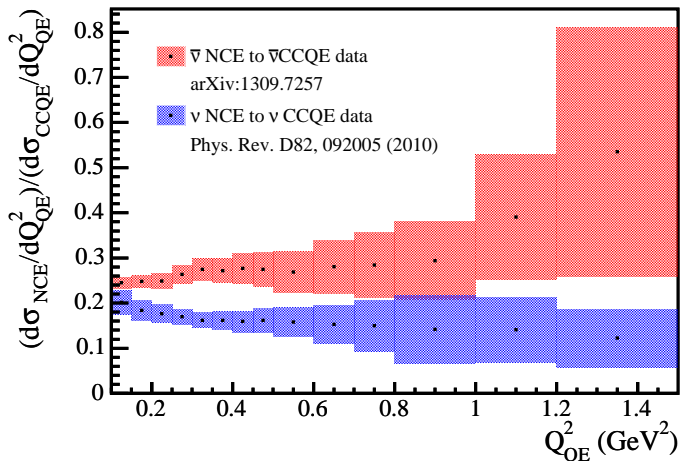


Figure 13: The MiniBooNE measured $(d\sigma_{NCE}/dQ_{QE}^2)/(d\sigma_{CCQE}/dQ_{QE}^2)$ cross section ratio for neutrino and antineutrino mode. The errors are dominated by systematics, i.e. statistical errors are small.

4.2 Dark Matter-Nucleon Sensitivities with Neutrino and Antineutrino Data

MiniBooNE has already published a detailed analysis of the neutral current nucleon neutrino cross sections dependent on 6.5×10^{20} POT [27] in neutrino mode, and 10.9×10^{20} POT in antineutrino mode [28]. The reconstructed nucleon kinetic energy was required to be less than 650 MeV and the reconstruction efficiency is 35%. The backgrounds came from various neutrino induced reactions such as neutrino interactions in the dirt, NCE-like events (NCE-pion where the pion is absorbed), and others. There were a total of 95,531 (60,605) NC events in neutrino (antineutrino) mode that were reconstructed with a purity of 65% (40%). The total systematic error was estimated at 18.1% (19.5%). There was no significant excess of events observed over the absolutely normalized Monte Carlo. Figure 14 shows the NC nucleon kinetic energy for data and Monte Carlo for both run modes.

We have performed a dark matter-nucleon scattering analysis on both the neutrino and antineutrino neutral current data sets. The neutrino data has half the POT and five times the neutrino background as the antineutrino mode, and hence is not as sensitive. Thus, we will only show the antineutrino analysis.

The dark matter-nucleon scattering fits included both energy and absolute RWM timing information. Figure 15 shows the nucleon energy data and 90% limits from the fits. The use of in-time improves the overall sensitivity by a factor of 1.5 for the low mass (shown). Slightly better exclusions are obtained for out-time fits in the high mass region (not shown). Clearly, with the huge neutrino backgrounds the sensitivity to the $g - 2$ region is poor. A better method is needed.

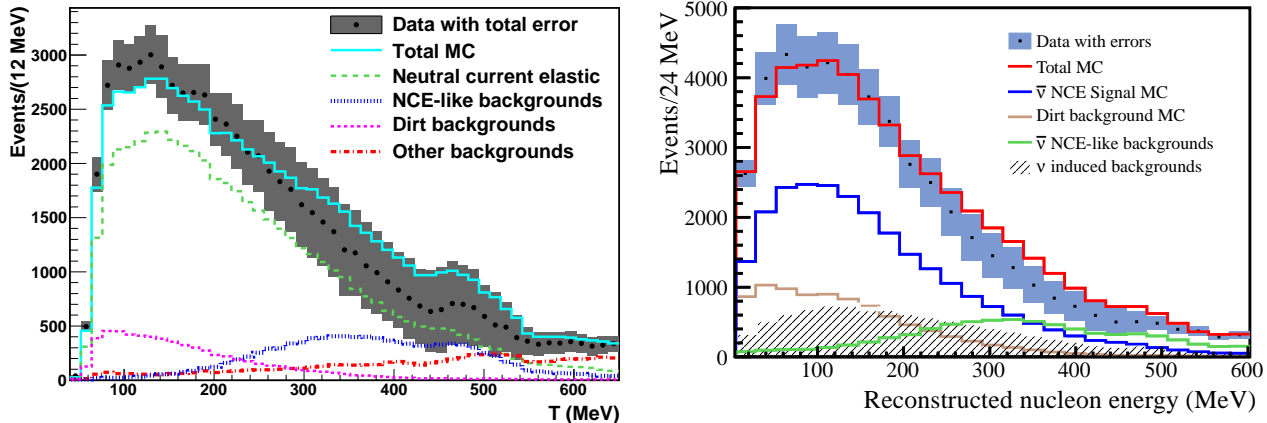


Figure 14: The NCE nucleon event reconstruction for 6.5×10^{20} POT in neutrino (left) and 10.9×10^{20} POT in antineutrino mode (right) [27]. The Monte Carlo is absolutely normalized to POT.

4.3 Dark Matter-Nucleon Sensitivities with One Week Beam Off Target Test Run

With the large number of backgrounds in normal beam-on-target mode, the limits are rather poor given the systematic errors at the $\sim 20\%$ level. The best way to improve these limits is to reduce the backgrounds from neutrino interactions. If we run in beam-dump mode with the 50 m absorber, then we can reduce the neutrino induced NCE events by a large factor.

A background that does not benefit from the beam-dump reduction are beam uncorrelated events from cosmic rays. For the neutral current elastic analysis this background is estimated at 0.5%. However, these events can be measured to high accuracy due to the large number of random (strobe) triggers that are taken throughout the run. These events can be subtracted off with little systematic error.

In May of 2012, a one week beam-dump run was performed to test the technical feasibility of a longer dark matter run. The beam-dump run collected 5.58×10^{18} POT, and was used to perform a low statistics dark matter analysis where many lessons were learned. One difference from the run proposed here is that the horn was on, resulting in twice the neutrino background event rate, i.e. a neutrino suppression of only 42.

The data was analyzed using calibrations and reconstruction from NCE analysis described above. The NCE event rate prediction was determined from the Monte Carlo where we tied the overall rate normalization to the measured CCQE muon neutrino rate in beam off target. The NCE nucleon rate is tied to the CCQE muon rate through the Fermi Gas cross section model with $M_A = 1.35$ [29, 30]. In beam-dump mode, and at low energies where NCE events reside, the cosmic and dirt backgrounds dominate. The beam unrelated cosmic background was measured using the random strobe trigger. The dirt was measured with high statistics in neutrino mode and then scaled by POT.

The reconstructed NCE event timing relative to the beam is shown in Figure 16, showing the event type breakdown and total backgrounds. Clearly, the beam unrelated cosmic and dirt backgrounds are significant for both in-time (6-14 nsec) and out-time (0-4 and 14-20

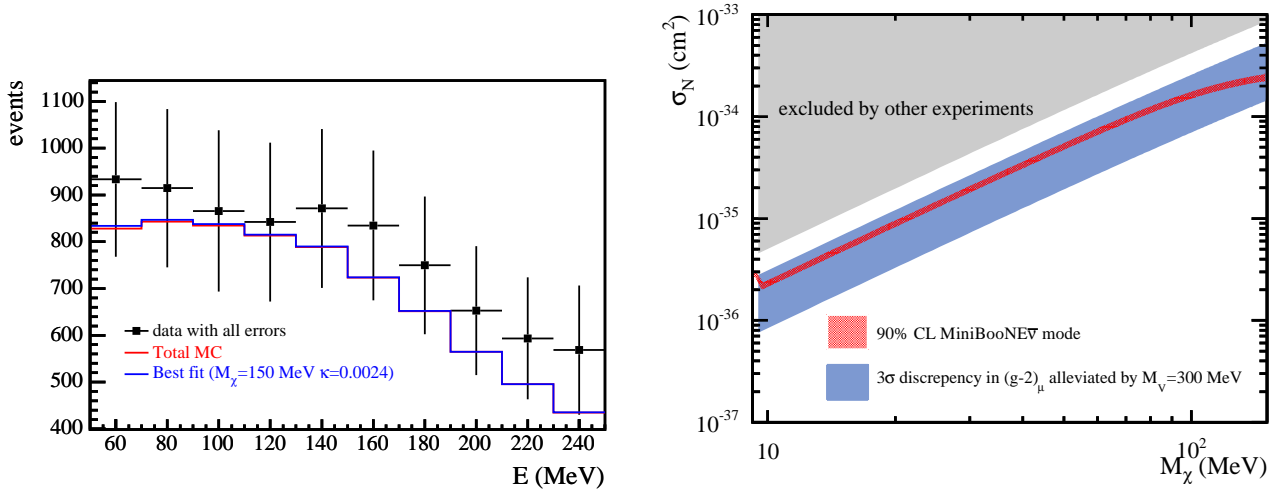


Figure 15: Dark matter-nucleon scattering fits to the antineutrino neutral current data set (10.9E20 POT). The plot on the left shows the reconstructed nucleon energy data (stat+sys error bars), absolutely normalized MC (red line), and best fit (blue line). The plot on the right is the resulting energy and in-time fit 90% exclusion limit (grey line) for the kinetic mixing coupling κ (related to cross section) versus dark matter mass (M_χ) parameter space.

nsec), while neutrino related NCE background dominates in-time. Making a simple time cut can enhance low mass dark matter searches (0-70 MeV) in-time and heavier dark matter searches (70-150 MeV) out of time. This was one of the important lessons learned with the beam-dump test run and use of timing. Clearly, fitting to dark matter-nucleon scattering timing distribution will give the maximum sensitivity, but for the purpose of understanding the effect, and a simple analysis, this works well.

The in-time and out-time energy distributions are shown in Figure 17 and event breakdown in Table 1. The systematic errors on the NCE are around 30% and come from the flux normalization and optical model. Systematic errors on dirt is 10%, and the strobe systematic errors is only 2% (though there is a sizable data statistical error contribution). Limits at the 90% CL have been generated that just touch on the upper part of the muon $g - 2$ band, a bit worse than the limits set in antineutrino mode. This is remarkable given that the data set is only 0.5% of the antineutrino data and shows the power of the beam-dump method to reject NCE backgrounds.

It will be shown in the next section that improvements in the large systematic errors are achieved with the use of the $(d\sigma_{NCE}/dQ_{QE}^2)/(d\sigma_{CCQE}/dQ_{QE}^2)$ constraint that is provided by the neutrino and antineutrino cross section measurements.

4.4 Projected Dark Matter-Nucleon Sensitivities with 0.35E20 POT and 1.75E20 POT in Beam-Dump mode: The Case for more Running

An important improvement realized for a dark matter search is constraining the NCE background event rate to the measured CCQE muon event rate, thereby significantly reducing

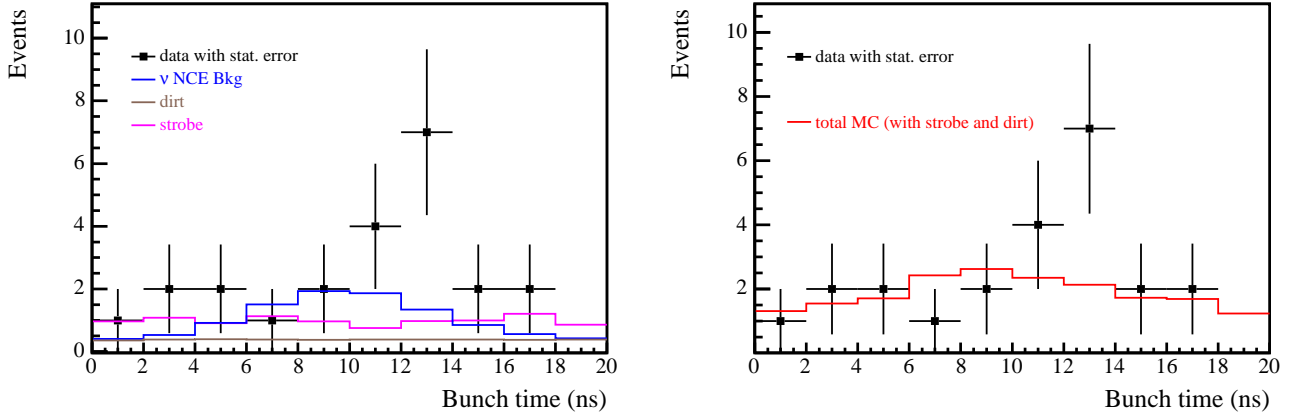


Figure 16: Data and MC event timing relative to the RWM for the one week test beam-dump run (5.58×10^{18} POT and horn on). On the left shows the various background components, and on the right the total background. Error bars are the data and are statistical only.

Event Type	In-Time (4-16 nsec)	Out-Time (0-4 and 16-20 nsec)
Data	24	5
NCE	9.3	1.4
Dirt	1.0	0.8
Cosmic	6.5	4.7
Total Background (stat/sys errors)	$16.8 \pm 4.1 \pm 3.0$	$6.8 \pm 2.6 \pm 0.6$
Data-Background (stat/sys errors)	$7.2 \pm 4.1 \pm 3.0$	$-1.8 \pm 2.6 \pm 0.6$

Table 1: Reconstructed NCE nucleon data and backgrounds for 5.5×10^{18} beam-dump (horn on) running for 50-600 MeV, and event Radius ≤ 4 m. Systematic errors are 30% on the NCE, 10% on dirt and 2% on strobe.

systematic errors in the background prediction (see Section 4.1.4). Other important backgrounds include beam unrelated cosmic events which are measured at a high rate (increased from 2 Hz to 15 Hz) with a random trigger. Dirt backgrounds are also significant but are tied to the neutrino flux, which is reduced in beam-dump mode, and is measured in both neutrino and antineutrino mode with a systematic error of 10%.

The event time of flight plays an important role in the simplest way by considering in-time and out-time regions to perform the energy fits. This allows a factor of two reduction in beam unrelated and dirt events for in-time, and a factor of six reduction of NCE events for out-time. A more sophisticated fit will use the dark matter-nucleon timing combined with energy distribution fits. This work is almost complete and might be available for the PAC meeting in January.

Putting everything together Figure 18 shows the expected dark matter-nucleon scattering sensitivity for 0.35×10^{20} POT and the requested 1.75×10^{20} POT. The improved analysis and the increase in data results in 3σ coverage of the entire muon $g-2$ signal region. Also shown are the expected 5σ sensitivity coverage, which is not insignificant. The plots shown are for a vector mediator mass $M_V = 300$ MeV and $\alpha' = 0.1$. The choice of these representative

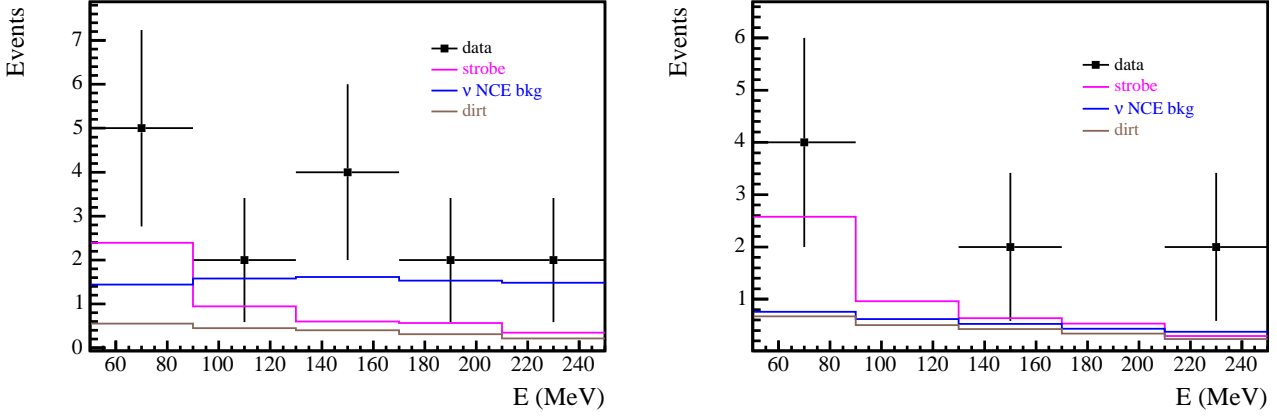


Figure 17: Data and MC reconstructed nucleon kinetic energy for the one week test beam-dump run (5.58×10^{18} POT) and horn on. On the left shows in-time events, and on the right out-time events. The the various Monte Carlo background components are shown as colored lines. Error bars are the data and are statistical only.

	0.35×10^{20} POT	0.35×10^{20} POT	1.75×10^{20} POT	1.75×10^{20} POT
Event Type	In-Time	Out-Time	In-Time	Out-Time
Data	-	-	-	-
NCE	54.9	10.9	274.6	54.7
Dirt	7.1	4.7	35.9	23.9
Cosmic	43.3	28.8	216.6	143.9
Total Background	$105.5 \pm 10.3 \pm 6.7$	$44.4 \pm 6.7 \pm 1.5$	$527.1 \pm 23.0 \pm 25.3$	$222.5 \pm 14.9 \pm 6.2$
Dark Matter Signal	67	45	275	221
Signal Significance	5.4σ	6.5σ	8.0σ	13.7σ

Table 2: Expected NCE nucleon and backgrounds for 0.35×10^{20} and 1.75×10^{20} POT in beam-dump mode. The dark matter number of events are for signal points along the center of the muon $g-2$ band. The first error on the total background is statistical and the second systematic.

parameters are discussed in the Section 3.

The event breakdowns, and errors for in-time and out-time are shown in Table 2. Also shown are the signal dark matter-nucleon rates along the center of the muon $g-2$ band. These give a sense of the signal size relative to backgrounds and errors, with the last row showing the significance. The individual systematic errors are 9% on NCE (12% for 0.35×10^{20}), 10% on dirt and 2% on cosmic (beam unrelated) backgrounds. The total statistical plus systematic errors are 15.2% for 0.35×10^{20} POT, and 9.9% for 1.75×10^{20} POT. The columns in-time (4-16 nsec) and out-time (0-4 and 16-20 nsec) are simple time cuts relative to the beam that enhances sensitivity to dark matter mass below 100 MeV, and above 100 MeV, respectively. The signal sensitivity for solutions along the center of the muon $g-2$ band are definitively covered above 5σ for 0.35×10^{20} POT or more.

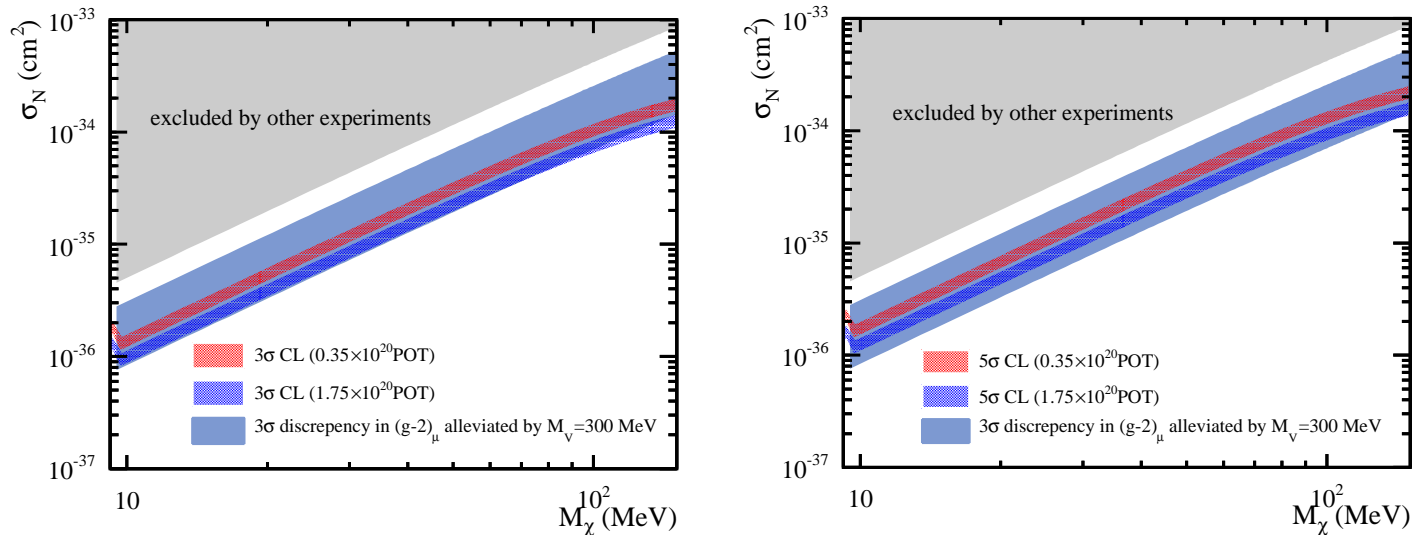


Figure 18: The cross section versus dark matter mass for the nucleon scattering channel for the beam-dump mode. MiniBooNE in-time estimated 3σ (left) and 5σ (right) C.L. upper limits for 0.35×10^{20} POT and 1.75×10^{20} POT are shown. The plot assumes a mediator mass $M_V = 300$ MeV, and $\alpha' = 0.1$. The width of the sensitivity lines represent the $\pm 25\%$ dark matter production errors.

4.5 Dark Matter-Electron Scattering Analysis

In the case of elastic scattering off electrons, we can make use of the kinematic fact that dark matter scattering will put the electron in a very forward direction with respect to the beam direction. In fact, the scattering angle with respect to the beam, θ_{beam} , will mostly satisfy $\cos \theta_{beam} > 0.99$ for dark matter scattering as well for electroweak neutrino-electron scattering. This is observable given that the MiniBooNE direction reconstruction sensitivity is 3 degrees [54], and a simple cut $\cos \theta_{beam} > 0.99$ reduces neutrino backgrounds by 98%. A more sophisticated analysis will fit the backgrounds and then extrapolate into the region $\cos \theta_{beam} > 0.99$ to estimate the signal. This method has the advantage of not relying on the Monte Carlo for background estimations, and hence, significantly reduces systematic errors.

Currently we do not have a detailed analysis of the dark matter-electron scattering analysis due to the fact that the current oscillation electron analysis has a 140 MeV lower energy threshold. Much of the anticipated electrons from dark matter scattering would have an energy below this threshold. In order to extract the most sensitivity requires much work to lower the energy threshold. The current particle identification needs to be verified at this lower energy, and the copious Michel electron rate needs to be handled. We have identified a team of collaborators who have taken on this job, and are already making good progress. We anticipate the ability to analyze this channel sometime in the next six months.

5 Experiment Turn On, Test Run Goals, and Collaboration Strength

The BNB (Booster Neutrino Beamline) and MiniBooNE detector were off during the recent year and a half FNAL accelerator shutdown. The BNB was recently turned back on in the early fall of 2013 to ensure it is running normally and ready for MicroBooNE running in 2014. After a month of repairing broken ion pumps, and fixing vacuum leaks, beam was successfully re-established. Also, the new beam multiwires which were installed during the shutdown were successfully commissioned and the new fiber RWM beam timing system was commissioned as well. This was accomplished with a short test run after the beamline was turned on. Also, the MiniBooNE detector was operated in order to take 5.5×10^{18} POT in antineutrino mode. This allowed a comparison of the target, horn, and decay pipe region performance to before the long shutdown. Figure 19 shows the results of this run where the reconstructed muon CCQE rate and energy was found to be consistent with antineutrino running before the shutdown. It has also been noted that before MicroBooNE turns on, it would be desirable to take a approximately one month high statistics neutrino run to check that that neutrino flux is identical to the flux MiniBooNE observed during its neutrino run. It is an important systematic check for MicroBooNE, since it will be a brand new detector and target (LAr) which will require some time to shake down and understand before it can verify the flux itself.

It should be noted that if a significant beam-dump NCE nucleon excess is observed during the proposed run, the background systematics can be changed in a controlled fashion by deploying the 25 m absorber and running for about three months. The 25 m absorber will reduce the neutrino flux and backgrounds by a factor of two, thus enhancing the signal significance. This action would only be proposed should there be strong motivation from the data.

After the antineutrino test run was completed by the beginning of November 2013, the BNB was configured to run in beam-dump, mode to collect 0.35×10^{20} POT. This run will allow MiniBooNE to collect enough statistics in this mode to improve the determination of the the neutrino flux reduction, which is an important input to the analysis. Also, the extra data will allow us to test the analysis methods we have proposed, which will decrease systematic errors significantly. At the time of the writing of this proposal we have collected about 0.22×10^{20} POT, and will run till we reach our goal. It is our aim to analyze this data and present the results at the PAC, to demonstrate that the new analysis method works, and delivers the expected sensitivity.

The success of the run and analysis requires a minimum number of personnel to staff shifts on a continual basis, and perform the low level data checks and high level physics analysis. At the time of the 2012 PAC proposal, we had 25 collaboration members willing to perform shift duties and analysis at fractional time. In the last year, due to the gaining awareness and interest in the physics of proton fixed target searches for light mass dark matter, our collaboration strength has increased. We now project 40 members with 5 new institutions added, and five participating theorists, three of which are full fledged collaboration members. The collaboration is also becoming international with institutions from Canada, Mexico, and the UK joining.

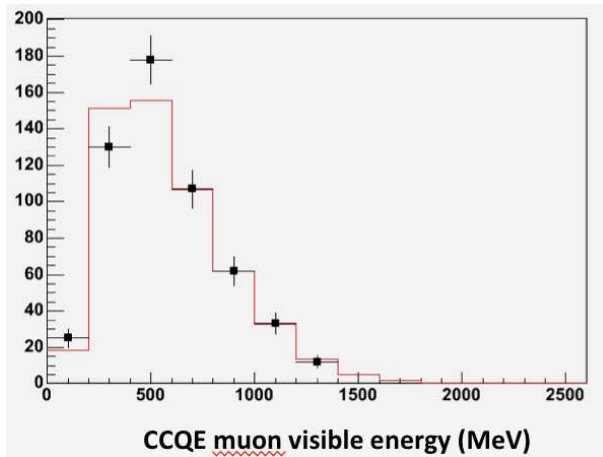


Figure 19: Reconstructed muon CCQE events from the recent antineutrino test run (data) compared to high statistics antineutrino rates before the shutdown (red line). The plot shows that after the shutdown the muon CCQE event rate and energy distribution are consistent, indicating the BNB target, horn, and decay pipe are working normally.

With 40 collaborators currently signed up, the shift burden will be about two 12 hour shifts a month. Given that the run is at most eight months in length (starting in the Fall of 2013), and the high level of interest in the run itself, this is not considered too much of a burden. Furthermore, remote shifting was enabled four years ago that allows shifters to take shifts from remote institutions. This has been instrumental in allowing off-site personnel to continue shift duties and participation in the experiment.

The cost of running the beamline is small, and continued running of the BNB is desired to ensure it is operating normally and ready for MicroBooNE running. It has been determined by Accelerator Division that running in beam-dump mode is safe and not considered a risk, especially since the beam does not impact the Be target and the horn remains off.

6 Summary

MiniBooNE has an unprecedented opportunity to search for dark matter. For certain models of light sub-GeV dark matter interacting via a light mediator which dominantly couples to quarks, MiniBooNE will have superior sensitivity in comparison to all other probes. In models based on hypercharge kinetic mixing, the sensitivity overlaps with a possible explanation of the muon $g - 2$ discrepancy as well as the observed relic abundance. This powerful probe of light dark matter is achieved by directing the beam past the target and onto the 50 m absorber, where neutrino production and thus the neutral current background rate is dramatically reduced, enhancing the sensitivity to dark matter or other exotic physics. We have described a variety of handles that will be exploited to enhance the sensitivity of this search to new physics contributions to neutral current - like signals, including nucleon energy shape, event timing, and the precise NCE/CCQE cross section ratio measurement.

It should be emphasized that this proposal, for concreteness, presented an interpretation of the search sensitivity for a particular dark matter model. However, the measurement of the beam-dump neutral current nucleon rate, which is highly constrained by the neutrino and antineutrino measured CCQE muon rates, provides a sensitive test of deviations from the Standard Model in a model-independent fashion, and can be straightforwardly interpreted in a variety of other new physics contexts.

MiniBooNE has the capability to perform this analysis in a timely manner. The collaboration will harness the last decade of work for this search, including the particle identification and higher analysis tools, extensive studies of the detector response, and relevant neutrino cross sections measurements. MiniBooNE has a proven track record of delivering on its goals, both operationally and with publications. For minimal cost and running until the middle of 2014, MiniBooNE can collect 1.75×10^{20} POT and obtain important new limits on sub-GeV dark matter. This is the first search of its kind, and the lessons learned will help to motivate a future program of dark matter searches with a suite of present and proposed FNAL experiments and accelerators.

7 The Request

MiniBooNE requests running to collect a total of 1.75×10^{20} POT in beam-dump mode. This will allow a sensitive measurement of the neutral current elastic nucleon event rate in a beam configuration mode that enhances any possible non-Standard Model contribution, with significant sensitivity to specific models of light dark matter in a parameter region consistent with the required cosmic relic density an explanation of the muon $g - 2$ discrepancy. The experiment further requests that this beam be delivered in 2014 before the MicroBooNE experiment turns on.

References

- [1] R. Dharmapalan *et al.* [MiniBooNE Collaboration], arXiv:1211.2258 [hep-ex].
- [2] R. Essig, J. A. Jaros, W. Wester, P. H. Adrian, S. Andreas, T. Averett, O. Baker and B. Batell *et al.*, arXiv:1311.0029 [hep-ph]; C. Adams *et al.* [LBNE Collaboration], arXiv:1307.7335 [hep-ex]; A. S. Kronfeld, R. S. Tschirhart, U. Al-Binni, W. Altmannshofer, C. Ankenbrandt, K. Babu, S. Banerjee and M. Bass *et al.*, arXiv:1306.5009 [hep-ex];
- [3] C. Athanassopoulos *et al.*, Phys. Rev. Lett. **75**, 2650 (1995); **77**, 3082 (1996); **81**, 1774 (1998); Phys. Rev. C. **58**, 2489 (1998); A. Aguilar *et al.*, Phys. Rev. D **64**, 112007 (2001).
- [4] A. A. Aguilar-Arevalo *et al.* [MiniBooNE Collaboration], arXiv:1207.4809 [hep-ex].
- [5] B. Batell, M. Pospelov and A. Ritz, Phys. Rev. D **80**, 095024 (2009) [arXiv:0906.5614 [hep-ph]].
- [6] P. deNiverville, M. Pospelov and A. Ritz, Phys. Rev. D **84**, 075020 (2011) [arXiv:1107.4580 [hep-ph]].
- [7] P. deNiverville, D. McKeen and A. Ritz, Phys. Rev. D **86**, 035022 (2012) [arXiv:1205.3499 [hep-ph]].
- [8] K. M. Zurek, arXiv:1308.0338 [hep-ph].
- [9] B. Batell, P. deNiverville, D. McKeen, M. Pospelov, and A. Ritz, *to appear*.
- [10] J. Goodman, M. Ibe, A. Rajaraman, W. Shepherd, T.M. Tait, et al., Phys. Rev. D **82**, 116010 (2010), [arXiv:1008.1783 [hep-ph]]; P.J. Fox, R. Harnik, J. Kopp, and Y. Tsai, Phys. Rev. D **84**, 014028 (2011), [arXiv:1103.0240 [hep-ph]]; A. Rajaraman, W. Shepherd, T. M. Tait, and A.M. Wijangco, Phys. Rev. D **84**, 095013 (2011), [arXiv:1108.1196 [hep-ph]]; P.J. Fox, R. Harnik, J. Kopp, and Y. Tsai, Phys. Rev. D **85**, 056011 (2012), [arXiv:1109.4398 [hep-ph]]; I.M. Shoemaker and L. Vecchi, (2011), arXiv:1112.5457 [hep-ph].
- [11] R. Essig, J. Mardon, and T. Volansky, (2011), arXiv:1108.5383 [hep-ph]; P.W. Graham, D.E. Kaplan, S. Rajendran, and M.T. Walters, (2012), arXiv:1203.2531 [hep-ph].
- [12] Y. Kahn and J. Thaler, arXiv:1209.0777 [hep-ph];
B. Wojtsekhowski, D. Nikolenko and I. Rachek, arXiv:1207.5089 [hep-ex].
- [13] C. Boehm, D. Hooper, J. Silk, M. Casse and J. Paul, Phys. Rev. Lett. **92**, 101301 (2004) [astro-ph/0309686].
- [14] N. Prantzos, C. Boehm, A. M. Bykov, R. Diehl, K. Ferriere, N. Guessoum, P. Jean and J. Knoedlseder *et al.*, arXiv:1009.4620 [astro-ph.HE].
- [15] B. W. Lee and S. Weinberg, Phys. Rev. Lett. **39**, 165 (1977).
- [16] C. Boehm and P. Fayet, Nucl. Phys. B **683**, 219 (2004) [hep-ph/0305261].
- [17] P. Fayet, Phys. Rev. D **70**, 023514 (2004) [hep-ph/0403226]
- [18] M. Pospelov, A. Ritz and M. B. Voloshin, Phys. Lett. B **662**, 53 (2008) [arXiv:0711.4866 [hep-ph]].
- [19] P. Gondolo and G. Gelmini, Phys. Rev. D **71**, 123520 (2005), [arXiv:hep-ph/0504010 [hep-ph]]; D.P. Finkbeiner and N. Weiner, Phys. Rev. D **76**, 083519 (2007), [arXiv:astro-ph/0702587 [astro-ph]]; D. Hooper and K.M. Zurek, Phys. Rev. D **77**, 087302 (2008), [arXiv:0801.3686 [hep-ph]]; N. Arkani-Hamed, D.P. Finkbeiner, T.R. Slatyer, and N. Weiner, Phys. Rev. D **79**, 015014 (2009), [arXiv:0810.0713 [hep-ph]]; M. Pospelov and A. Ritz, Phys. Lett. B **671**, 391 (2009), [arXiv:0810.1502 [hep-ph]].

- [20] P. Fayet, Phys. Rev. D **75**, 115017 (2007) [hep-ph/0702176 [HEP-PH]].
- [21] M. Pospelov, Phys. Rev. D **80**, 095002 (2009) [arXiv:0811.1030 [hep-ph]].
- [22] B. Batell, M. Pospelov, and A. Ritz, Phys. Rev. D **79**, 115008 (2009), [arXiv:0903.0363 [hep-ph]]; R. Essig, P. Schuster, and N. Toro, Phys. Rev. D **80**, 015003 (2009), [arXiv:0903.3941 [hep-ph]]; M. Reece and L.-T. Wang, JHEP **0907**, 051 (2009), [arXiv:0904.1743 [hep-ph]]; J.D. Bjorken, R. Essig, P. Schuster, and N. Toro, Phys. Rev. D **80**, 075018 (2009), [arXiv:0906.0580 [hep-ph]]; P. Schuster, N. Toro, and I. Yavin, Phys. Rev. D **81**, 016002 (2010), [arXiv:0910.1602 [hep-ph]]; R. Essig, P. Schuster, N. Toro, and B. Wojtsekhowski, JHEP **1102**, 009 (2011), [arXiv:1001.2557 [hep-ph]]; R. Essig, R. Harnik, J. Kaplan, and N. Toro, Phys. Rev. D **82**, 113008 (2010), [arXiv:1008.0636 [hep-ph]]; J. P. Lees *et al.* [BABAR Collaboration], Phys. Rev. Lett. **108**, 211801 (2012) [arXiv:1202.1313 [hep-ex]].
- [23] V. Barger, C. -W. Chiang, W. -Y. Keung and D. Marfatia, Phys. Rev. Lett. **106**, 153001 (2011) [arXiv:1011.3519 [hep-ph]]; D. Tucker-Smith and I. Yavin, Phys. Rev. D **83**, 101702 (2011) [arXiv:1011.4922 [hep-ph]]; B. Batell, D. McKeen and M. Pospelov, Phys. Rev. Lett. **107**, 011803 (2011) [arXiv:1103.0721 [hep-ph]].
- [24] J. L. Hewett, H. Weerts, R. Brock, J. N. Butler, B. C. K. Casey, J. Collar, A. de Gouvea and R. Essig *et al.*, arXiv:1205.2671 [hep-ex].
- [25] A.A. Aguilar-Arevalo *et al.*, Phys. Rev. D **83**, 052009 (2011).
- [26] A.A. Aguilar-Arevalo *et al.*, Phys. Rev. D **83**, 052007 (2011).
- [27] A.A. Aguilar-Arevalo *et al.*, Phys. Rev. D **82**, 092005 (2010).
- [28] A.A. Aguilar-Arevalo *et al.*, arXiv:1309.7257 [hep-ex] (2013).
- [29] A.A. Aguilar-Arevalo *et al.*, Phys. Rev. D **81**, 092005 (2010).
- [30] A.A. Aguilar-Arevalo *et al.*, Phys. Rev. D **88**, 032001 (2013).
- [31] A.A. Aguilar-Arevalo *et al.*, Phys. Rev. D **81**, 013005 (2010).
- [32] A.A. Aguilar-Arevalo *et al.*, Phys. Rev. Lett. **103**, 081801 (2009).
- [33] A.A. Aguilar-Arevalo *et al.*, Phys. Lett. B **664**, 41 (2008).
- [34] A.A. Aguilar-Arevalo *et al.*, Phys. Rev. Lett. **100**, 032301 (2008).
- [35] B. Holdom, Phys. Lett. B **166**, 196 (1986).
- [36] A. A. Aguilar-Arevalo *et al.* [MiniBooNE Collaboration], Phys. Rev. D **79**, 072002 (2009) [arXiv:0806.1449 [hep-ex]].
- [37] L. B. Auerbach *et al.* [LSND Collaboration], Phys. Rev. D **63**, 112001 (2001) [hep-ex/0101039].
- [38] A. Hook, E. Izaguirre and J. G. Wacker, Adv. High Energy Phys. **2011**, 859762 (2011) [arXiv:1006.0973 [hep-ph]].
- [39] B. Aubert *et al.* [BaBar Collaboration], arXiv:0808.0017 [hep-ex].
- [40] E. Izaguirre, G. Krnjaic, P. Schuster and N. Toro, arXiv:1307.6554 [hep-ph].
- [41] R. Essig, J. Mardon, M. Papucci, T. Volansky and Y. -M. Zhong, JHEP **1311**, 167 (2013) [arXiv:1309.5084 [hep-ph]].

- [42] G. Angloher, S. Cooper, R. Keeling, H. Kraus, J. Marchese, Y. A. Ramachers, M. Bruckmayer and C. Cozzini *et al.*, *Astropart. Phys.* **18**, 43 (2002).
- [43] J. Angle *et al.* [XENON10 Collaboration], *Phys. Rev. Lett.* **107**, 051301 (2011) [arXiv:1104.3088 [astro-ph.CO]].
- [44] I. M. Shoemaker and L. Vecchi, *Phys. Rev. D* **86**, 015023 (2012) [arXiv:1112.5457 [hep-ph]].
- [45] M. Ablikim *et al.* [BES Collaboration], *Phys. Rev. Lett.* **100**, 192001 (2008) [arXiv:0710.0039 [hep-ex]].
- [46] J. Barreto *et al.* [DAMIC Collaboration], *Phys. Lett. B* **711**, 264 (2012) [arXiv:1105.5191 [astro-ph.IM]].
- [47] R. Agnese *et al.* [CDMSlite Collaboration], arXiv:1309.3259 [physics.ins-det].
- [48] D. S. Akerib *et al.* [LUX Collaboration], arXiv:1310.8214 [astro-ph.CO].
- [49] M. S. Atiya, I. H. Chiang, J. S. Frank, J. S. Haggerty, M. M. Ito, T. F. Kycia, K. K. Li and L. S. Lit-tenberg *et al.*, *Phys. Rev. Lett.* **69**, 733 (1992).
- [50] A. V. Artamonov *et al.* [E949 Collaboration], *Phys. Rev. Lett.* **101**, 191802 (2008) [arXiv:0808.2459 [hep-ex]].
- [51] L. B. Auerbach *et al.* [LSND Collaboration], *Phys. Rev. D* **63**, 112001 (2001) [hep-ex/0101039].
- [52] H. An, X. Ji and L. -T. Wang, *JHEP* **1207**, 182 (2012) [arXiv:1202.2894 [hep-ph]].
- [53] S.A. Ouedraogo, "Limit on the Muon Neutrino Magnetic Moment and a Measurement of the CCPIP to CCQE Cross-Section Ratio", PhD Thesis, Louisiana State University, 2008
- [54] R. B. Patterson, E. M. Laird, Y. Liu, P. D. Meyers, I. Stancu and H. A. Tanaka, *Nucl. Instrum. Meth. A* **608**, 206 (2009) [arXiv:0902.2222 [hep-ex]].